Stability Limit Guidelines for Superconducting Coil Design

P.L. Walstrom

January 1985

UWFDM-611

FUSION TECHNOLOGY INSTITUTE

UNIVERSITY OF WISCONSIN

MADISON WISCONSIN

Stability Limit Guidelines for Superconducting Coil Design

P.L. Walstrom

Fusion Technology Institute
University of Wisconsin
1500 Engineering Drive
Madison, WI 53706

http://fti.neep.wisc.edu

January 1985

UWFDM-611

STABILITY LIMIT GUIDELINES FOR SUPERCONDUCTING COIL DESIGN

Peter L. Walstrom

Fusion Technology Institute

Nuclear Engineering Department

University of Wisconsin

Madison, WI 53706

March 1985

UWFDM-611

ABSTRACT

As a guide to non-specialists in the field of superconductivity, curves for the limiting current density for various methods used for stabilizing superconducting coil windings are presented as a function of field for Nb_3Sn and NbTi superconducting current carrying elements at various temperatures. The curves represent the approximate guidelines on limits on current density imposed by stability only, and for large magnet systems, protection and mechanical considerations may further reduce the allowable current density.

1. Introduction

The superconducting coil designer has available a range of options in designing a coil winding pack. For coils of moderate size (e.g. the 0.5 meter base EBT-P prototype coils)[1] metastable windings permeated with 1 atm, 4.2 K liquid helium for transient stability provide a high current density, cost effective approach. Coil designers have been reluctant, however, to use metastable designs for larger systems due to their low stability, and, in fact, most existing large superconducting magnets are cryostable. Two other design approaches of especially recent interest are the force-flow, internally cooled cable superconductor (ICCS) and superfluid helium (He-II) cooled windings. To date, experience with large coils of the latter two types is limited. The LCP program in Oak Ridge is expected to provide test data on three large (3 m diameter) force-flow coils together with three cryostable bath cooled coils; one force-flow coil (the Euratom-KfK coil) has been tested alone to a self-field of about 5 T. The Tore II-Supra device at CEN-Saclay, France will provide operating experience with He-II cooled coils in an experimental tokamak plasma confinement device of moderate size (coils approximately 2 meters diameter) and peak field (9 T). The major limitation of the large coil tests when compared to requirements of present day fusion reactor studies is the relatively low peak test field of 8 T; for example, the Westinghouse coil, which has Nb_3Sn superconductor, is mechanically limited to currents considerably below its calculated stability margin.

2. Metastable Windings

The curves for metastable windings are shown in Fig. 1 mainly for comparison purposes because the stability of this winding approach is generally considered too low for application in large, high-field coils. The three

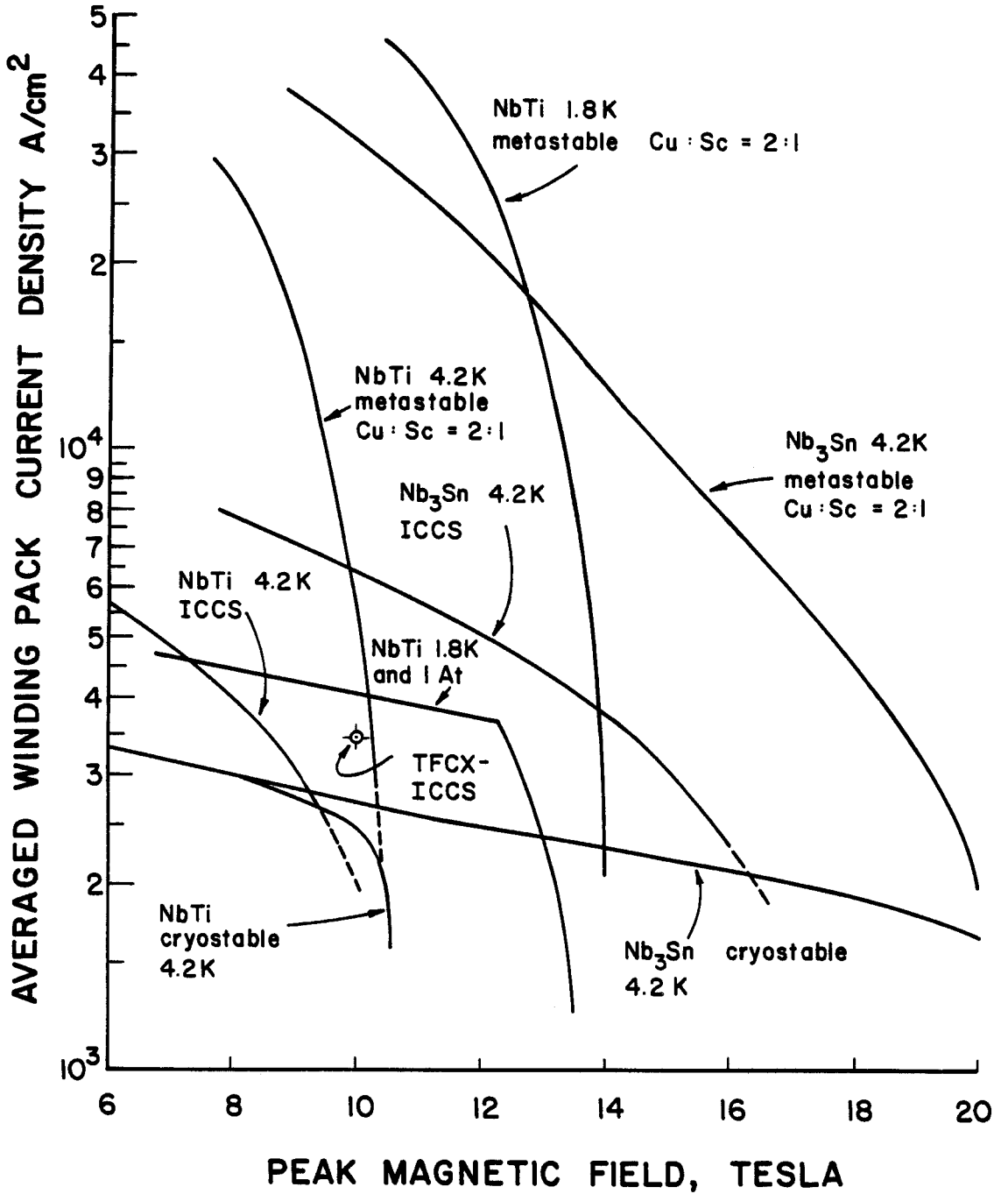

Fig. 1. Stability-limited winding pack current densities for various stabilization methods. See text for detailed explanations of assumptions to derive the individual curves.

curves for metastable windings were generated simply by multiplying published current density data for the superconductor fraction (or more properly speaking, the non-copper fraction) of the best commercially available superconducting material by a constant factor. That is, the winding pack density j_p is taken to be

$$j_p(B,T) = \lambda\, f_{sc}\, j_c(B,T)\ , \qquad (1)$$

where λ is the metal fraction in the winding, f_{sc} is the non-copper fraction in the superconducting composite, and $j_c(B,T)$ is the current density averaged over the non-copper fraction of the composite. A value of 0.8 was assumed rather arbitrarily for λ (this means 20% of the pack is helium and insulator); a 2:1 copper to superconductor ratio was chosen, which gives $f_{sc} = 0.33$.

In deriving the above-described stability limit curves as well as the following ones, for NbTi at 4.2 K the data of Kwang and Larbalestier[2] for Nb 50.4 Ti were used. For NbTi at 1.8 K, the data of M. Wake et al. for the ternary alloy NBTiTa (19 w/o Ta) were used.[3] Finally, for Nb_3Sn at 4.2 K, the data of Suenaga et al. for Nb_3Sn + Ti bronze process wire were used.[4] In all cases the data represent high but commercially achievable current densities.

3. Cryostable Windings

In this basically conservative approach, sufficient normal metal is added to the composite (usually by soldering the composite into a copper element) and sufficient cooling provided by boiling liquid helium in cooling chambers so that the Joule power is less than the steady-state minimum boiling heat flux. For this reason, the more restrictive term, cryostatic stabilization,

is sometimes used for the above design approach. The attractive feature of cryostatically stabilized windings is that the designer need not know what the transient thermal disturbances will be, provided they are not so large that the coolant is blown out of large portions of the windings. The main problem in designing cryostatically stabilized windings is that the heat transfer characteristics of pool-boiling liquid helium are highly configuration-dependent and not amenable to analytic modeling. This is a result of the fact that the process of heat removal in the steady state depends on replenishment of helium liquid in the cooling channels. The driving force for replenishment flow is the buoyant force on the vapor-laden helium in the channels. The time required to set up such flows can be quite long - on the order of a second - compared to the duration of many transient disturbances (e.g. conductor movement, which occurs in milliseconds). As a result, in actual practice, the idealized cryostatic heat transfer condition may never be reached in recovery from a transient, if the heat input is not too large. Instead, recovery in these cases will take place by transient heat transfer to the helium in the channel at the time of the transient. For larger disturbances, for which the transient heat transfer is insufficient to absorb the energy, recovery will occur in a cryostatically stable winding after a delay of a second or so, as determined by replenishment of the helium initially in the channel. In such cases, it is possible for the heat transfer rate to be initially high during the transient phase, then drop as the conductor surface is vapor-blanketed, and again return to the somewhat higher steady-state value (but less than the value during the initial transient phase) as the replenishment current is established.

In should be clear from the above discussion that use of a fixed boiling heat transfer curve to analyze all configurations is at best a crude approximation and that use of constant heat transfer coefficient is cruder still. In fact, only for the small values of ΔT, the temperature difference between the conductor and the helium bath, in the nucleate boiling region is the heat transfer nearly configuration-dependent. This can be seen in Fig. 2, which is a plot of steady-state heat transfer curves[5] for a one-foot mockup of a section of the General Electric LCP coil instrumented with heaters and thermocouples. The various curves represent different angles of the conductor axis from the horizontal as would occur at various locations in the winding pack. (Horizontal is at the top and bottom of the coil and vertical at the equatorial plane of the coil.) Shown for comparison is a "typical" curve for steady-state liquid helium boiling heat transfer.[6] The curves for the various orientations coincide only for the low values of ΔT in the nucleate boiling region. The worst heat transfer occurs when the conductor is horizontal, in which case the channels in which the bulk of the heat is deposited are horizontal. The best heat transfer occurs in the vertical axis case, in which the channels are highly inclined. In this case, the heat transfer is actually better than the "typical" curve in the film boiling region and is enhanced by the so-called "chimney" effect - buoyancy-driven circulation and associated heat transfer in an inclined channel open at the top and bottom.

Analogous heat transfer data were published for winding mockup tests of the General Dynamics LCP coil.[7,8] They are characterized by generally better heat transfer performance than the GE windings (due to the lack of long horizontal heated channels) and a marked but different angular dependence.

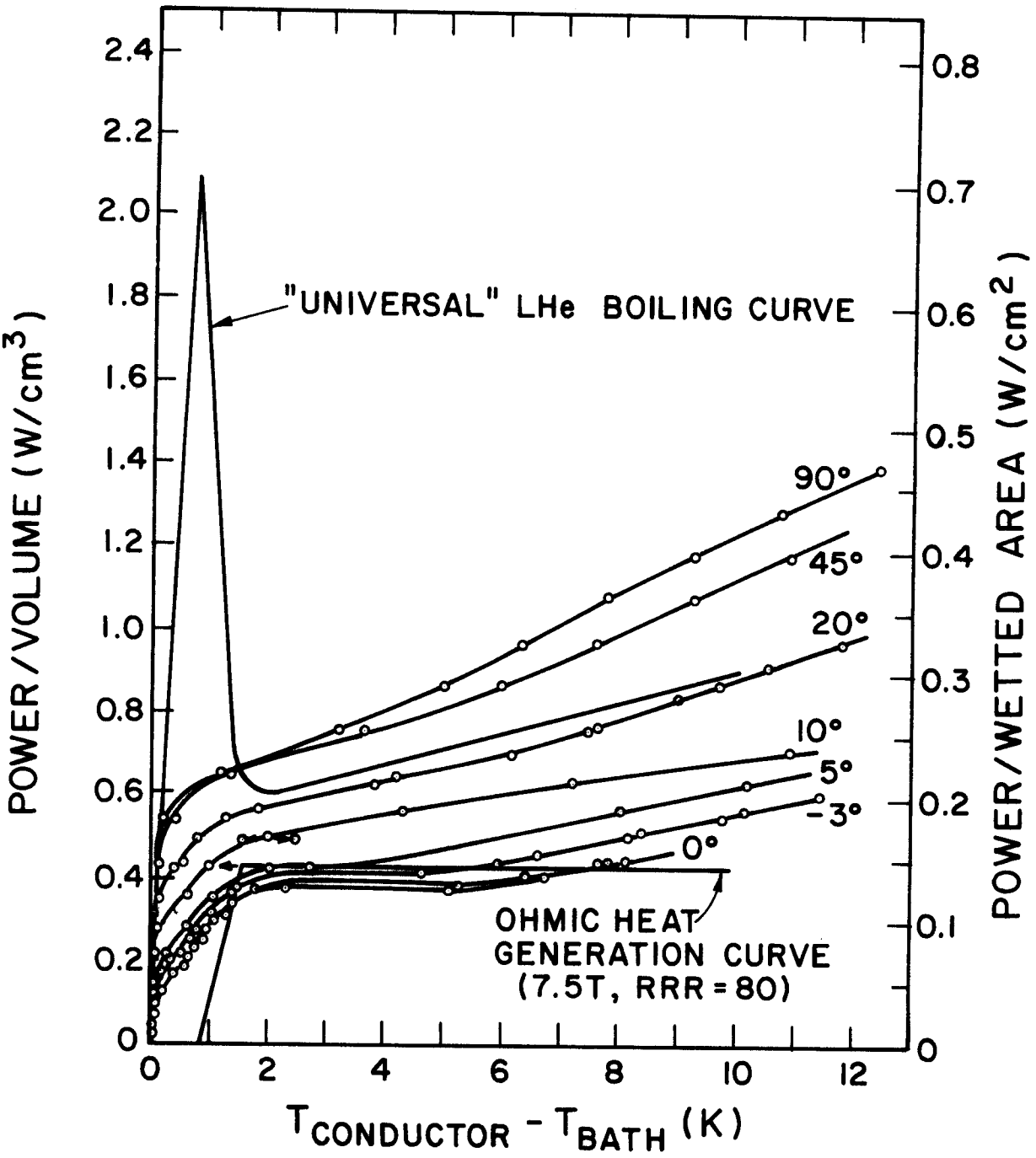

Fig. 2. Measured steady-state heat removal in saturated 4.2 K He-I from a mockup of the General Electric LCP coil winding pack at various inclinations of the conductor axis from the horizontal. Shown for comparison is a "typical" heat transfer curve.

In setting guidelines for cryostability limits for future magnets, then, the only reasonable approach thus appears to be to scale from existing empirical data on winding pack heat-removal performance, as indicated either by mockup tests, or, if available, results from heated turns in magnets. The highest current-density, demonstrably cryostatically stable winding pack densities for large, high-current coils in the 8 T range which the author was able to find were in the GD and JA LCP coils and the MFTF-A magnet. Data for the GD windings are taken from the mockup tests of Ref. 7 and 8. These data yield an unconditional stability limit for the GD/LCP coil with a peak field at 8 T of 2950 A/cm^2 averaged over the winding pack. In the calculation, magnetoresistance was taken into account, but not radiation degradation. Also, conductor grading was taken into account. A similar calculation for the GE LCP magnet based on the data of Ref. 5 yields an unconditional stability limit of only 2400 A/cm^2 in the worst orientation under the same conditions, a value less than the design current density. This coil, then, must recover by cold-end conduction in these regions when at design current. Data for the Japanese LCP coil were taken from the single-coil domestic test,[9] in which recovery of normal zones initiated by heaters was studied at various currents. By extrapolation of the latter data and taking into account the magnetoresistances at the extrapolated single-coil field (6.4 T) and the design field for array testing (8 T), a limiting current density of 2850 A/cm^2 was obtained. Finally, for MFTF, normal zone recovery data from the MFTF test coil,[10] a solenoid wound with the MFTF-A conductor, yield a limiting winding pack current density of 3000 A/cm^2. However, this value is for cold-end recovery. If unconditional stability is required, the data indicate a current density of only 2500 A/cm^2 is allowable. The above results are summarized in Table 1.

Table 1. Cryostability Data for Four Large Coils Cooled by Pool-Boiling Helium

Coil	J_{design} (A/cm^2)	Minimum heat flux removed/wetted surface (W/cm^2)	Heat flux generated at design current (W/cm^2)	J_{limit} (A/cm^2)
GD-LCP	2600 in high-field region 2740 overall	0.17	0.15	2950
GE-LCP	2400 in high-field region 2500 overall	0.13	0.14	2500
JA-LCP	2400 in high-field region 2600 overall	0.58*	0.42	2850
MFTF	3000	0.19*	0.19	3000† 2500

* Extrapolated from domestic test results, Ref. 9. with a correction for the magnetoresistance.

† Value for cold-end recovery.

The best performance is in the neighborhood of 3000 A/cm^2. This is an optimistic figure and a practical upper limit for copper-stabilized coils at 8 T, especially if higher-current conductors are to be used, as it is difficult to maintain a high cooled surface area per conductor cross-section as the cross-section increases.

In generating the curves for the cryostability limit in Fig. 1, account was taken of two factors which affect the achievable current density. The first is the magnetoresistance. The stabilizer was assumed to be copper, and an empirical expression from the MARS study[11] was used to calculate the magnetoresistance. The resistivity ρ_B at field is given by the formula

$$\rho(B) = \rho(o) \left[1 + 4.37 \left(\frac{B}{\rho(o) \times 10^9}\right)^{1.115}\right] \qquad (2)$$

where $\rho(o)$ is the resistivity at zero field in ohm-cm, and B is the field in tesla. The second effect taken into account is the fact that in a superconducting-normal metal composite area must be provided for superconductor and at fields approaching the upper critical field, the superconductor area must increase rapidly in order that the composite remain superconducting. The latter constraint is not usually involved explicitly in plots of I vs. B, which show the stability limit curve intersecting the critical current curve. For the cryostability limit curves in Fig. 1, the two constraints, carrying the critical current and producing an ohmic heating flux not to exceed the heat removal capability, were combined. It was assumed implicity that the winding pack geometry remains unchanged (and therefore the heat removal and metal fraction are constant), but more superconductor is added as the field increases to keep the critical current equal to the operating current. This, of course, yields

a limiting curve and actual designs would have more superconductor in order to keep the operating current somewhat below the critical value. Denoting the winding pack current density at the 8 T point from which we scale by j_o and the current density at other fields by j, then we have

$$\frac{\rho(8\ T) j_o^2}{f_{cu}^o} = \frac{\rho_B j^2}{f_{cu}} \ . \tag{3}$$

Where f_{cu} is the copper fraction and ρ_B is the resistivity at field B. If we further denote the metal fraction (copper plus superconductor) in the cross-section by f_m, and if we assume the superconductor is at the critical current,

$$j = j_c(1 - f_{cu})\ f_m \ . \tag{4}$$

Combining (3) and (4), one has,

$$\frac{\rho_o}{f_{cu}^o}\ j_o^2 = \frac{\rho_B j^2}{1 - \frac{j}{j_c f_m}} \ . \tag{5}$$

Equation (5) is a quadratic equation which can be solved for j, the limiting current density. In deriving the curves for Fig. 1 from Eq. (3), a current density of 3000 A/cm^2 at 8 T was assumed, and GD/LCP coil copper and metal fractions were used. Also, the fact that the superconductor at the 8 T scaling point is carrying less than the critical current was neglected. The error due to the above approximation is small due to the high copper to superconductor ratio at the 8 T reference point.

It may be noted that at high fields where the critical current is approaching zero, the metastable curves actually intersect the cryostable curves. What has happened here is that the cryostable design as defined by Eq. (5) actually has more superconductor and less copper than the metastable design above the intersection of the curves.

Finally, it should be noted that use of high purity aluminum rather than copper for all or part of the stabilizer could improve the high-field performance considerably, with an especially large improvement above 10 T with the Nb_3Sn curve. It yet remains to be seen if the drawbacks (low elastic modulus, low yield strength) of pure aluminum in combination with brittle Nb_3Sn can be overcome in large magnet systems.

4. Internally Cooled Cable Superconductor (ICCS)

Stability in a cable-in-conduit superconducting current-carrying element is dependent upon mass flow rate and current, and also on pulse time, length of the heated zone, helium pressure, and on the magnetic field via stabilizer resistivity and superconductor critical temperature. In most designs considered to date, supercritical helium at a pressure of about 5 atmospheres is favored for thermodynamic reasons. Although boiling liquid helium can provide even greater stability, the pumping requirement through long passages make its use prohibitive in most applications. For this reason, 6 atm supercritical helium at 4.2 K will be assumed. Results can be approximately scaled to different temperatures by use of the scaling formula given later in this section.

The stability margin is defined as the maximum pulse energy per unit metal volume of the cable inside the conduit which can be absorbed with subsequent recovery to the superconducting state. The stability margin for a

particular ICCS forms a surface in three dimensions when plotted against mass flow and current.[12] An interesting feature of the surface is that it is folded; this fact means that for a certain region in the $\dot{M}$, I plane, the stability is multi-valued. This region is bordered on one side by the line of zero mass flow and extends to a limiting mass flow value which corresponds to a velocity of about 50 cm/s. Above the limiting mass flow the stability is single-valued regardless of the current. In the region of multi-valued stability, as the pulse energy is increased from zero, the conductor is first stable up to a value called the lower stability margin, then unstable for a range of pulse energies, stable again for a range of energies, then finally unstable above an upper stability margin. For mass flows less than the critical value, the stability margin is single-valued and large (on the order of 500 MJ/cc) if the current is below a value called the limiting current, which forms the lower I value boundary of the region of multiple stability in the $\dot{M}$, I plane. The multiple stability behavior is caused by heating-induced flow which enhances the heat-transfer coefficient. For magnet systems, the limiting mass flow is often too high from a point of view of optimizing the cryogenic system and a lesser flow, just enough to remove steady-state heat, is used. In this case, in order to avoid the region of multiple stability, in which only the lower stability margin of about 30 MJ/cc can be depended upon, the current is kept below the limiting current. The limiting current density therefore sets the limit for stable operation of the coil and is the quantity plotted in Fig. 1 for ICCS magnets.

The pulse energy which can be absorbed by an ICCS below the limiting current is given by the approximate expression[13]

$$\Delta H \cong \frac{1 - f_m}{f_m} \int_{T_B}^{T_{cs}} \rho c_p dT \qquad (6)$$

where f_m is the metal fraction inside the conduit, T_B is the bath temperature, T_{cs} is the current-sharing temperature, ρ is the helium density, and C_p is the helium specific heat. Equation (6) is simply a statement that for recovery, the helium can absorb only enough energy to bring it to the current sharing temperature. If the temperature of the helium exceeds the current sharing temperature, recovery cannot occur because replenishment of heated helium by cold helium is negligible on the time scale of the recovery process. Equation (6) is approximate because the pressure rise is neglected and also because the fact that the helium can do work on helium upstream and downstream is neglected.

Based on a series of experiments mainly performed on miniature cables of three wires in capillary tubes (triplexes), Lue, Miller, and Dresner[14,15] developed an empirical scaling relation for the limiting current. The scaling relation is based on a semi-quantitative theory developed by Dresner.[12,14,16] Their relationship is

$$J_{lim} \sim [f_{cu} f_m (1 - f_m)]^{1/2} \, (T_c(B) - T_b)^{1/2} \, \rho(B)^{-1/2} \tau^{-1/15} \ell^{2/15} D^{-1} \qquad (7)$$

where J_{lim} is the current density averaged over the interior of the conduit, f_{cu} the copper fraction in the composite wires, f_m the fraction of metal in the conduit, $T_c(B)$ the critical temperature at field B, T_b the coolant temperature before the pulse, $\rho(B)$ the normal metal resistivity, τ the pulse length, ℓ is the heated length, and D the hydraulic diameter. The exponents for J and ℓ are taken from Reference 17 rather than from Reference 12. The copper to

superconductor ratio was taken to be 1.5:1 and the void fraction $(1 - f_m)$ was taken to be 0.40. An overall packing fraction $\lambda = j_{pack}/j_{conduit}$ of 0.8 was assumed. For the critical temperature T_c of NbTi, the formulae[18]

$$T_c = 9.2\ [1 - B/14.5]^{0.59} \qquad B < 10\ T$$

and (8)

$$T_c = 8.96\ [1 - B/14.8]^{0.59} \qquad B > 10\ T$$

were used (B in tesla, T_c in kelvin). For the critical temperature of Nb_3Sn, the expression of Hudson et al. was used.[19] Equation (2) was used again to calculate the resistance of the copper at field with an assumed residual resistance ratio of 100. The heated length and pulse length were assumed to be the same as for the triplex data from which the limiting current was scaled[14,15], namely, 3.25 m and 5 ms, respectively. Furthermore, a correction was made[20] for the fact that in triplexes the conduit wall contributes to friction but not to heat transfer, while in a large ICCS the conduit wall area can be neglected compared to the surface area of the wires. This amounts to replacing D^{-1} in Eq. (7) with $D_f^{-1/2} D_h^{-1/2}$, where D_f is the hydraulic diameter calculated with the conduit wall perimeter and D_h the hydraulic diameter without the wall perimeter. No attempt was made to stability-optimize the conductor by varying the copper-to-superconductor ratio and void fraction, because the void fraction is limited to the value used for mechanical reasons and the copper to superconductor ratio by conductor manufacturing considerations. Finally, it should pointed out that Eq. (7) can be converted from a proportionality expression to an equation by setting a pressure-dependent coefficient in front of the expression given. It turns

out[20] that the coefficient is a fairly slowly varying function of pressure in the range of interest and is within ten or fifteen percent of unity if SI units are used in the formula. For the curves in Fig. 1, the pressure was assumed to be the same as for the experiments from which the limiting current was scaled, namely, 5 atmospheres.

The $\ell^{2/15}$ dependence of J_{lim} on the length of the normal zone in Eq. (7), though weak, implies that J_{lim} approaches zero as the length of the heated zone approaches zero, i.e., that the conductor is less stable to short-length disturbances than to longer disturbances. This trend is the opposite of that observed in cryostability. The above result is plausible in that heating-induced flow should be reduced in shorter heated lengths; however, for some sufficiently short lengths, end conduction should again raise the stability. It may be, therefore, that there is a shallow minimum in the stability curve as a function of length. It is possible, also, that for some minimum length the stability surface will lose its fold and become everywhere single-valued; in this case the concept of limiting current loses any meaning. Questions of this sort plus the fact that Eq. (7) is based largely on triplex data rather than full-sized cable data demonstrates the need for further systematic experiments with full-size NbTi and Nb_3Sn ICCS conductors at various temperatures with heated lengths varying from the ICCS diameter to the length of a single turn in a large coil (i.e. 20 m or so) and with varying unheated lengths up to those corresponding to a single helium circuit in a large coil (say 100 m).

5. Superfluid Helium-Cooled NbTi Windings

The use of superfluid helium (He-II) offers the designer the combined advantages of higher critical field and critical currents than at 4.2 K and the enhanced heat transfer capabilities of He-II. With use of the ternary alloy NbTiTa, operating in fields up to 12.5 T is feasible.

In most large He-II cooled magnet systems proposed to date, a coolant temperature around 1.8 K and pressure of 1 atm were chosen. The latter pressure is many times the saturation pressure of helium at 1.8 K, 0.02 atm; as a result, if vapor is formed, it is converted back to liquid. The dominant heat removal mechanism in pressurized He-II is therefore conduction through the liquid, not buoyancy-driven flow as in the case of He-I on the saturation curve. Fortunately, the effective thermal conductivity of He-II is much greater than that of He-I. Reviews of the general subject of heat transfer in He-II can be found in References 16 and 21.

In the steady-state* recovery of a conduction from a temperature above the bath temperature is limited by either the temperature gradient in the channels removing heat from the conductor or by the Kapitza thermal resistance at the boundary between the fluid and the conductor. Heat transport in the channels is governed by the non-linear Gorter-Mellink law:

$$q = - K\left(\frac{dT}{dx}\right)^{1/3} . \qquad (9)$$

---

* In practice, steady-state cooling is not available because it would require an infinite He-II reservoir at the end of the channel. The expression derived below is appropriate for low heat flux designs typical of large magnets; for a discussion of high heat flux transient stability, see Ref. 23.

The effective thermal conductivity, according to this law, is proportional to the heat flux cubed if K is assumed to be temperature-independent. Typically, $K \sim 10\ W\ cm^{-5/3}\ K^{-1/3}$. When a conductor is driven normal (say $T > 10$ K) a film of He-I vapor and liquid is formed on the surface; in order for this film to be converted back to He-II and recovery to take place, the temperature rise due to Gorter-Mellink conduction in He-II in a channel of constant cross-section must not exceed $T_\lambda - T_b$, where T_λ is the HeI-HeII transition temperature and T_b is the bath temperature. Otherwise, the He-I layer will grow and recovery will never occur. The resultant equation is

$$\left(\frac{q}{K}\right)^3 = -\frac{dT}{dx} = \frac{T_\lambda - T_b}{\ell} \tag{10}$$

where ℓ is the channel length.

It is assumed in the above that the temperature at the end of the channel is fixed at T_b. In most magnet windings, channels are cross-connected, so more conduction area is available as the distance from the conductor increases. As a result, effective channel lengths are shorter than would be the case for parallel unbranched channels and somewhat high fluxes can be tolerated. Typical steady-state channel fluxes determined by Eq. (10) are on the order of a few watts per square centimeter; when referred to the conduction surface, they are again on order of a few watts per centimeter squared.

The second criterion for recovery in the quasi-static approximation is related to the Kapitza heat flux q_k, given by the empirical expression

$$q_k = A(T^n - T_b^n) \tag{11}$$

where T is the conductor temperature. In general, the Kapitza resistance limits the stable current density at high fields, while the channel conduction limits it at lower fields.

Following the analysis of Dresner,[22] the Kapitza - conductance limited heat flux can be determined by the relationship of the heat generation curve to the heat removal curve, given in this case by Eq. (11) (see Fig. 3). For recovery in the quasi-static approximation, the heat removal at every temperature must exceed the heat generation (cold-end recovery is not considered). There are four possible situations, depending upon the value of i, the ratio of operating current to critical current.

For i = 1, the current sharing temperature T_{cs} equals T_b and the maximum heat flux q_m (the height of the flat top region of the heat generation curve) is determined by the slope of the q_k curve at T_b:

$$q_m(1) = nAT_b^{n-1} (T_c - T_b) . \tag{12}$$

For somewhat lower values of i, q_m is determined by the condition that the heat generation curve be tangent to the q_m curve. The lowest value of i for this zone is reached when the heat generation curve is tangent to the q_k curve at T_c. Denoting the corresponding value of i by i_o, one has

$$\frac{q_m(i_o)}{T_c - T_{cs}(i_o)} = nAT_c^{n-1} \tag{13}$$

using the fact the slopes are equal at T_c. Also, one has the relation

$$q_m(i_o) = A(T_c^n - T_b^n) \tag{14}$$

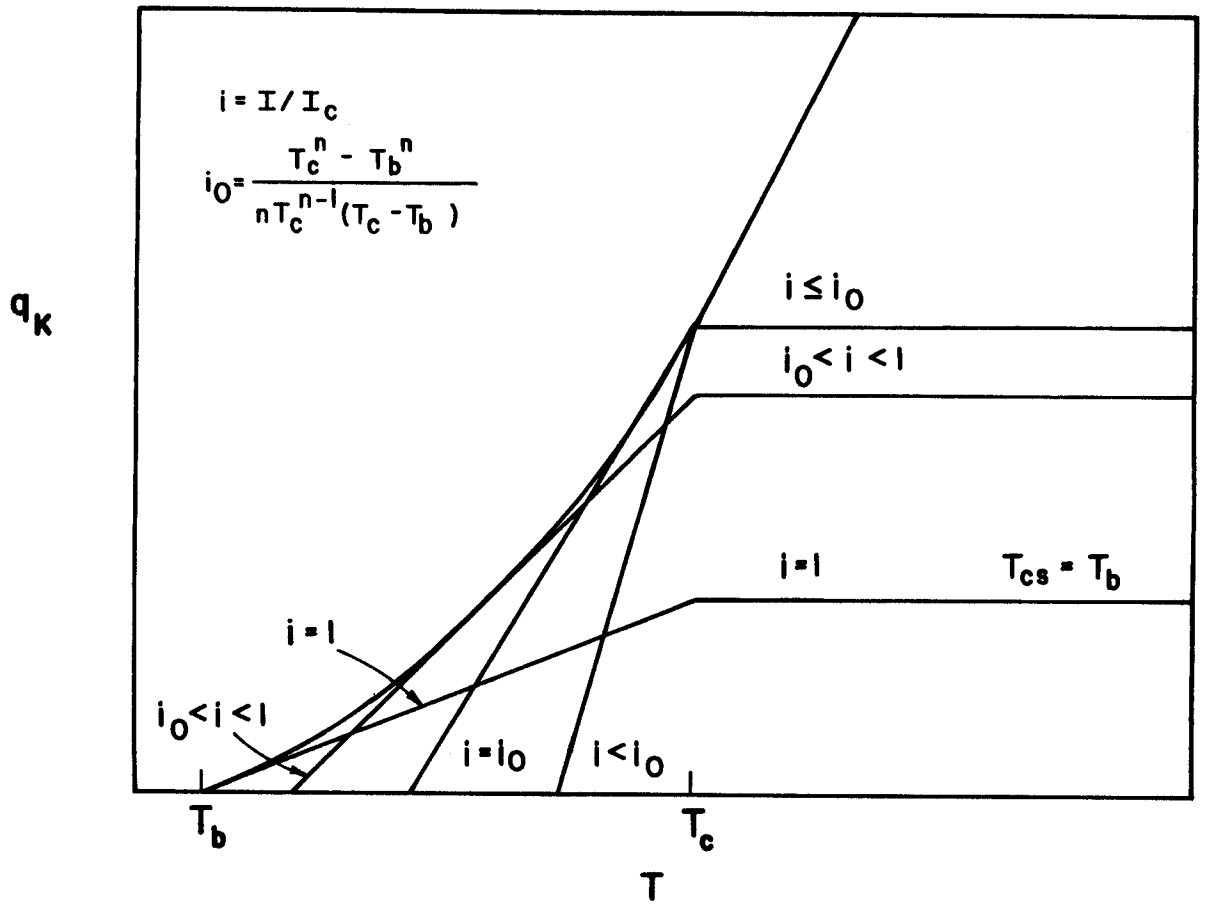

Fig. 3. Relationship of the Kapitza heat conducting curve to Joule heat generation curves for various values of i, the ratio of operating to critical current.

and the customary relation between current sharing temperature and critical temperature:

$$T_c - T_{cs}(i) = i(T_c - T_b) \ . \tag{15}$$

Combining Eqs. (13), (14), and (15), one gets for i_o

$$i_o = \frac{T_c^n - T_b^n}{nT_c^{n-1}(T_c - T_b)} \ . \tag{16}$$

For values of i still lower than i_o, q_m is unchanged from that at i_o (see Fig. 2).

For values of i between i_o and 1, q_m is larger than the value q_o of the heat flux at the point of tangency (see Fig. 2), i.e.,

$$q_m(i) = q_o\left(\frac{T_c - T_{cs}}{T_o - T_{cs}}\right) \ . \tag{17}$$

Denoting $T_{cs} - T_b$ by ΔT, one has, using (15)

$$q_m = q_o \frac{i\Delta T}{T_o - T_c + i\Delta T} \ . \tag{18}$$

Also, one has from the equality of slopes

$$nAT_o^{n-1} = \frac{q_m(i)}{i\Delta T} \tag{19}$$

and from (12)

$$q_o = A(T_o^n - T_b^n) \quad . \tag{20}$$

Combining (17), (18), and (20), the following equation for $q_m(i)$ is obtained:

$$(\frac{n-1}{n})(ina\Delta T)^{-\frac{1}{n-1}} q_m^{\frac{n}{n-1}} + (i\Delta T - T_c)\, q_m + iA\Delta T T_b^n = 0 \quad . \tag{21}$$

Eq. (21) can be solved numerically for q_m as a function of i if exact values are required. It can be easily shown by partial differentiation of Eq. (21) and use of Eqs. (13-16) that the slope of $q_m(i)$ vs. i is zero at i_o; q_m can thus be approximated by a parabola for values of i close to i_o; i.e.

$$q_m \cong q_m(i_o) - a\,(\frac{i - i_o}{i_o})^2 \quad . \tag{22}$$

It is easily shown by substitution in (21) that

$$a = \frac{nAT_c^n}{2(n-1)} \quad . \tag{23}$$

For the purpose of determining the limiting current density curve, the value of i which gives the highest current density for each value of magnetic field is desired. This is equivalent to adjusting the copper to superconductor ratio at each field to give the maximum current, since the metal fraction and conduction cross-section are considered fixed. One has

$$i = \frac{I}{I_C} = \frac{j}{j_c f_m (1 - f_{cu})} \quad . \tag{24}$$

The heat generation for a given copper fraction

$$q = \frac{A_c \rho_B}{f_m^2 p} \frac{j^2}{f_{cu}} \tag{25}$$

where A_c is the conductor cross-section and P the average wetted perimeter. Using (24) to eliminate f_{cu}, one obtains

$$q = \frac{A_c \rho_B}{f_m^2 P} \frac{j^2}{1 - \frac{j}{i f_m j_c}} . \tag{26}$$

Eq. (26) can then be solved for j. The positive root is the one sought. Defining

$$\alpha_B = \frac{f_m^2 P}{A_c \rho_B} \tag{27}$$

one obtains for j the expression

$$j = (q_m \alpha_B)^{1/2} \left[\left(1 + \frac{q_m \alpha_B}{(2 i f_m j_c)^2}\right)^{1/2} - \frac{(q_m \alpha_B)^{1/2}}{2 i f_m j_c} \right] . \tag{28}$$

The job is now to maximize j as a function of i, remembering that q_m is itself a function of i. This can be done numerically; the results for j differ little (less than a percent) from the values calculated using q_o. In view of the large scatter in curves for q_k reported in the literature, then, a sufficiently accurate procedure in practice is to calculate q_m from Eq. (14) and substitute it in Eq. (28).

In calculating the curve for NbTi at 1.8 K in Fig. 1, Eq. (28) with a fixed value of q_m of 1 watt/cm^2 was used for the low field region. Values of

0.5 for f_m, 8 cm for P and 2.0 cm^2 for A_c were chosen. Values for A and n in Eq. (11) were chosen to be 0.028 and 3.3, respectively; these represent an average curve for copper.[23] The change in slope in the curve is the point where the Kapitza flux is equal to the value assumed for the channel-limited flux - 1 watt/cm^2; above this field the current density is Kapitza-flux limited; below it, it is channel-flux limited.

6. Other Considerations Affecting Current Density

Two other factors affecting the maximum stable current density in magnets are mechanical forces and protection considerations. The stress analysis of a magnet including the winding pack is a formidable one because of the composite nature of the windings and the complicated boundary and load conditions. From the limited point of view of the winding pack, however, some simple scaling rules do apply. For magnets with long straight legs, such as D-shaped tokamak toroidal magnets, the radial compression loads in the straight sections cannot be carried by loop tension and are transmitted directly through the stack to the outer ring. In this case, radial stress scales as B^2 and is given approximately by the "magnetic pressure" expression

$$\sigma_r = \frac{B^2}{2\mu_o} . \tag{29}$$

At 10 T, for example, this yields 40 MPa or 5800 psi, which is the yield point for soft copper. In some pool-boiling winding designs with transverse channels, the radial stress can be larger than the average value because the conductor is not everywhere supported. In ICCS winding packs, the high stress occurs in the sides of the square conduit which must carry the compression forces.[24] In both cases, the situation can be alleviated by adding steel

appropriately to carry the loads. The end result is a lower current density. The curves in Fig. 1 can be modified to reflect addition of steel by multiplying by the quantity f_m'/f_m, where f_m' is the copper plus superconductor fraction in the winding pack with added steel, and f_m is the value used in calculating the curves of Fig. 1 (see text). Similar considerations apply to windings limited by loop tension. In this case, the appropriate approximate formula is

$$\sigma_t = jBr \ . \tag{30}$$

At B = 10 T, j = 3 x 10^7 A/m^2, and r = 2 m, this yields 600 MPa or 87,000 psi, considerably above the yield strength of even hard copper. This means that either steel must be co-wound with the conductor turns or most of the radial load must be taken by radial compression. In the latter case, we are back to Eq. (28). Therefore, steel must be added either to carry the hoop tension or to take the radial compression and the average current density is lowered correspondingly.

Another constraint on the allowable current density is protection considerations. In stabilized magnets, most of the energy is removed by an external dump resistor during an emergency discharge and the dump time is dominated by the external resistance R and the coil inductance L:

$$I(t) = I_o e^{-\frac{tR}{L}} \tag{31}$$

where I_o is the coil current at the start of the dump and I(t) is the current during the dump. The temperature of a "hot spot" - a length of conductor in

the normal state at the beginning of the dump - is determined by ohmic heating and heat transfer to the coolant during the dump.

For a length of the conductor, neglecting end conduction, one has

$$S(T)\ A_c \frac{dT}{dt} = I^2 \frac{(t)\ \rho(t)}{A_c} - Pq(t)\ . \tag{32}$$

Where S(T) is the volume specific heat and the other quantities are as previously defined. The resistivity is written as $\rho(T)$ without dependence on B because after the temperature has exceeded about 30 K the magnetoresistance is negligible compared to the zero-field resistance. Dividing through by A_c, and writing Eq. (32) in terms of the winding pack current density, one obtains

$$S(T) \frac{dT}{dt} = \frac{j^2(t)\ \rho(T)}{f_m^{\ 2}} - \frac{P}{A_c} q(t)\ . \tag{33}$$

The difficulty in solving (33) is our ignorance of the cooling term $q(t)P/A_c$. In pool-boiling coils, the difficulty is that we don't know the helium temperature and velocity and effective heat transfer during a dump. The situation is similar in a He-II cooled magnet, because local zones of He-I liquid and vapor could be formed. A conservative approach taken in many analyses is to set q(t) equal to zero; this overestimates the hot spot temperature. With the foregoing approximation, Eq. (3) can be readily solved:

$$\int_{T_i}^{T_f} \frac{S(T)}{\rho(t)}\, dT = \frac{j_o^{\ 2}}{f_m^{\ 2}} \int_o^{\infty} e^{-\ tR/L}\, dt = \frac{j_o^{\ 2}}{f_m^{\ 2}} \frac{L}{R}\ . \tag{34}$$

The left-hand side of Eq. (34) can be written in terms of the antiderivative of the quantity inside the integral sign; denoting it by F, one has

$$F(T_f) - F(T_i) = \frac{j_o^2 L}{f_m^2 R} . \tag{35}$$

The allowable current density can then be written in terms of the desired final temperature

$$j_o = f_m \left[F(T_f) - F(T_i)\right]^{1/2} \left(\frac{R}{L}\right)^{1/2} . \tag{36}$$

The function F(T) can be determined numerically from materials properties data.

The designer is faced here with a set of tradeoffs. He can decrease the dump time L/R and according to Eq. (36) increase the allowable current density. If R is increased, the dump voltage $I_o R$ is increased and the likelihood of electrical breakdown and arcing somewhere in the magnet system is increased. For a given magnet stored energy, which scales as the peak magnetic field squared times a linear dimension cubed, the only way to reduce L is to increase the current and decrease the number of turns, leaving the ampere-turns constant. However, high-current conductors are harder to manufacture, are harder to stabilize, require larger power supplies, leads, and switchgear, etc. For very large systems, such as magnetic energy storage devices, use of external dump resistors is not feasible and dumping the energy in the winding themselves by rapidly warming them in the only available practicable protection mode.

In analysis of ICCS protection, one approach which has been taken is to replace C_p for the conductor in Eq. (3) with a C_p for copper plus helium, with specific assumptions about the state of the helium during the dump (usually

that the pressure is constant at the maximum design value and the density decreases by mass expulsion from the ends of the conduit). This yields a somewhat lower final temperature or a higher allowable current density.

As an illustration of the above, the TFCX designers chose the design point shown in Fig. 1, which is considerably lower than that set by stability of the ICCS Nb_3Sn conductor above. In this case, the limiting current set by stability scaled down by volume for structural steel was comparable to that for protection similarly scaled down. For larger systems, unless the operating current is increased, the limiting current density will be still lower and determined by protection.

Acknowledgement

Support for this work has been provided by the U.S. Department of Energy.

References

1. J.R. Miller, J.W. Lue, S.S. Shen, "Tests of First Development Coils for EBT-P," Proc. 9th Symp. on Engineering Problems of Fusion Research, IEEE Pub. No. 81CH1715-2 NPS (1981) p. 2012.

2. K.F. Kwang and D.C. Larbalestier, IEEE Transactions on Magnetics, Vol. May-15, No. 1 (1979) p. 400.

3. M. Wake et al., IEEE Transactions on Magnetics, Vol. May-15, No. 1 (1979) p. 400.

4. M. Suenaga, C.J. Klamut, N. Higuchi, and T. Kuroda, "Properties of Ti Alloyed Mutifilamentary Nb_3Sn Wires by Internal Tin Process", Proc. 1984 Applied Superconductivity Conf. (to be published in IEEE Transactions on Magnetics).

5. P.L. Walstrom, Advances in Cryogenic Engineering, Vol. 27, Plenum Press, NY (1982) p. 319.

6. The curve plotted is an average of the data shown in Fig. 6.3 of M.N. Wilson's book, Superconducting Magnets, Claredon Press, Oxford, (1983) p. 93.

7. E.H. Christianson, Proc. 8th Symp. on Engineering Probs. of Fusion Research, IEEE Pub. No. 79CH1441-5 NPS (1979) p. 1769.

8. E.H. Christianson and S.D. Peck, Advances in Cryogenic Engineering, Vol. 27, Plenum Press, NY (1982) p. 327.

9. S. Shimamoto et al., IEEE Transactions on Magnetics, Vol. May-19, No. 3, p. 855 (1983).

10. D.N. Cornish, J.P. Zbaznik, R.L. Leker, D.G. Hirzel, J.E. Johnston, and A.R. Rosdahl, IEEE Transactions on Magnetics, Vol. May-15, No. 1 (1979) p. 530.

11. UCRL-53480, "Final Report of Mirror Advanced Reactor Study," July 1984.

12. L. Dresner, IEEE Transactions on Magnetics, Vol. May-17, No. 1, (1981) p. 753.

13. J.R. Miller, Advances in Cryogenic Engineering, Vol. 27, p. 207, Plenum Press, NY (1982).

14. J.W. Lue, J.R. Miller, and L. Dresner, J. Appl. Phys. 51 (1) Jan. 1980, p. 772.

15. J.W. Lue and J.R. Miller, IEEE Transactions on Magnetics, Vol. May-17, No. 2 (1981) p. 257.

16. L. Dresner, Cryogenics, June 1984, p. 283.

17. J.W. Lue and J.R. Miller, "Heated Length Dependence of the Stability of an Internally Cooled Superconductor", Proc. 9th Symp. on Engineering Problems of Fusion Res., IEEE Pub. No. 81CH1715-2 NPS, New York (1981) p. 652.

18. M.S. Lubell, IEEE Transactions on Magnetics, Vol. May-19, No. 3, (1983) p. 754.

19. P.A. Hudson et al., IEEE Transactions on Magnetics, Vol. May-19, No. 3 (1983) p. 903.

20. J.R. Miller, private communication.

21. S.W. Van Sciver, Advances in Cryogenic Engineering.

22. L. Dresner, "A Rapid, Semi-Empirical Method of Calculating the Stability Margins of Superconductors Cooled with Subcooled He-II", 1984 (unpublished).

23. J. Adam et al., "Torus II Supra", EUR-CEA-FC-1021 (1979) (Euratom Report).

24. P. Materna, "Comprehensive Design Procedure and Spreadsheet for Internally Cooled Cabled Superconductors", Proc. 1984 Applied Superconductivity Conference, San Diego, Sept. 1984.